Membrane-active antimicrobial peptide identified in *Rana arvalis* by targeted DNA sequencing

Tomislav Rončević[a,*], Lucija Krce[a], Marco Gerdol[b], Sabrina Pacor[b], Monica Benincasa[b], Filomena Guida[b], Ivica Aviani[a], Vedrana Čikeš-Čulić[c], Alberto Pallavicini[b], Ana Maravić[d], Alessandro Tossi[b]

[a] *Department of Physics, Faculty of Science, University of Split, Croatia*
[b] *Department of Life Sciences, University of Trieste, Italy*
[c] *Department of Medical Chemistry and Biochemistry, School of Medicine, University of Split, Croatia*
[d] *Department of Biology, Faculty of Science, University of Split, Croatia*

ARTICLE INFO

Keywords:
Antibacterial activity
Aggregation
Anuran antimicrobial peptides
Membrane active peptides
Targeted DNA sequencing

ABSTRACT

Antimicrobial peptides (AMPs) are naturally produced, gene encoded molecules with a direct antimicrobial activity against pathogens, often also showing other immune-related properties. Anuran skin secretions are rich in bioactive peptides, including AMPs, and we have reported a novel targeted sequencing approach to identify novel AMPs simultaneously in different frog species, from small quantities of skin tissue. Over a hundred full-length peptides were identified from specimens belonging to five different Ranidae frog species, out of which 29 were novel sequences. Six of these were selected for synthesis and testing against a panel of Gram-negative and Gram-positive bacteria. One peptide, identified in *Rana arvalis*, proved to be a potent and broad-spectrum antimicrobial, active against ATCC bacterial strains and a multi-drug resistant clinical isolate. CD spectroscopy suggests it has a helical conformation, while surface plasmon resonance (SPR) that it may self-aggregate/oligomerize at the membrane surface. It was found to disrupt the bacterial membrane at sub-MIC, MIC and above-MIC concentrations, as observed by flow cytometry and/or visualized by atomic force microscopy (AFM). Only a limited toxicity was observed towards peripheral blood mononuclear cells (PBMC) with a more pronounced effect observed against the MEC-1 cell line.

1. Introduction

AMPs or host defense peptides (HDPs) are structurally diverse multifunctional effector molecules naturally produced by all organisms having a direct antimicrobial activity and/or immunomodulatory properties [1,2]. They are considered to be potential new therapeutic agents useful in a battle against the rapidly spreading multi-drug resistant bacteria [3], with many peptides in phase I–III of clinical phase of development [4,5]. However, there are a number of limitations in development of potential peptide antibiotics, resulting in only a handful of AMPs approved for clinical use to date. Some major concerns are low metabolic stability and short half-life (lability to proteases, serum, salt, pH), a tendency for aggregation, unacceptable toxicity and high production costs [4–6]. Nevertheless, AMPs are often membrane-active antibiotics, with a mechanism that is to a certain extent similar to that of colistin, which in recent years has been used as a “drug of last resort” against Gram-negative pathogens. However, its effectiveness could also become hindered due to reported cases of resistance [7], especially by plasmid-mediated dissemination of the *mcr-1* gene [8].

AMPs are an abundant source of novel potential antibiotics, and according to Data Repository of Antimicrobial Peptides (DRAMP) [9], 4851 AMPs with diverse structure and activity have been reported. Anurans, and in particular their skin secretions, are a rich source of such peptides [10]. Since the first frog peptide was identified from the

Abbreviations: DiOC6, 3,3′-dihexyloxacarbocyanine iodide; DOPC, 1,2-dioleoyl-*sn*-glycero-3-phosphocholine; DPPG, 1,2-dipalmitoyl-*sn*-phosphatidylglycerol; AFM, atomic force microscopy; AMPs, antimicrobial peptides; CD, circular dichroism; LUVs, large unilamellar vesicles; ORFs, open reading frames; SPB, sodium phosphate buffer; SDS, sodium dodecyl sulphate; SPR, surface plasmon resonance; TFA, trifluoroacetic acid; TFE, trifluoroethanol

* Corresponding author.
E-mail addresses: troncevic@pmfst.hr (T. Rončević), lkrce@pmfst.hr (L. Krce), mgerdol@units.it (M. Gerdol), pacorsab@units.it (S. Pacor), mbenincasa@units.it (M. Benincasa), milenaguida@gmail.com (F. Guida), iaviani@pmfst.hr (I. Aviani), vedrana.cikes.culic@mefst.hr (V. Čikeš-Čulić), pallavic@units.it (A. Pallavicini), amaravic@pmfst.hr (A. Maravić), atossi@units.it (A. Tossi).

Accepted 18 December 2018

skin secretions of *Xenopus laevis* in the late 1980s [11], numerous AMPs have been identified in most of anuran families (e.g. 1102 peptides deposited in DRAMP have been identified in frogs) and in particular in Ranidae [12]. Frogs from this family are known to secrete multiple active AMPs [12], which are likely expressed by relatively large gene families, as also confirmed by a study we recently carried out on five different species [13]. In the past, identifying novel anuran AMPs required handling a number of individuals which were stimulated by noradrenaline (e.g. norepinephrine) to obtain small amounts of crude peptide. Following initial fractionation by RP-HPLC, potential peptides were identified by activity testing of the obtained fractions. Active components were then purified, and the sequence determined by different methods, including mass spectrometry [14]. Although effective, this approach is very time consuming, and more importantly raises issues related to the ethical treatment of animals and to the protection of amphibian species which are often experiencing a sharp population decline due to habitat destruction and anthropic activities [15].

We have previously reported an alternative, high-throughput method for AMP identification which is faster, more efficient, less invasive and allows for simultaneous peptide identification from several individuals belonging to different species [13]. Implementing degenerate primers designed on the most conserved regions of AMP precursors, the signal sequence, allowed us to simultaneously identify 127 peptide sequences from five different Ranidae species, including 29 novel sequences. Six peptides were then selected for synthesis and tested for their antibacterial potential against a panel of Gram-negative and Gram-positive bacteria, including methicillin-resistant *Staphylococcus aureus*. The toxicity towards animal cells was examined on circulating human blood cells and the MEC-1 cell line. The peptides showed a quite variable antimicrobial activity, ranging from broad spectrum to selective or completely inactive, and antimicrobially active peptides were relatively nontoxic towards animal cells in vitro, at concentrations corresponding to their MIC or MBC. The most active peptides were examined for their ability to bind with the surface of model biological membranes and to perturbate or disrupt bacterial membranes. Based on surface plasmon resonance (SPR) results and CD spectra, it was possible to correlate the potency of the most active peptide to its ability to self-aggregate/oligomerize on interaction with the model or bacterial membranes, which could have also contributed to a moderate toxicity towards some types of host cells.

2. Materials and methods

2.1. Peptide identification and relatedness

Peptides were identified from different Ranidae species including *Pelophylax ridibundus*, *Pelophylax* kl. *esculentus*, *Rana dalmatina*, *Rana temporaria* and *Rana arvalis*, as described in detail in Roncevic et al. [13]. Briefly, complete RNA was extracted from ~50 mg of skin tissue. Simultaneously, signal peptide sequences belonging to Ranidae species were obtained from Database of Anuran Defense Peptides (DADP) [16], aligned and used to generate Hidden Markov Model (HMM) profiles. The RNAseq data available in the Sequence Read Archive (SRA) database [17] for Ranidae was then probed by using these HMM profiles and *de novo* assembled, enabling the identification of expressed sequences encoding for potential AMPs. Positively hit nucleotide sequences were aligned and grouped by similarity (> 80%) in three clusters, which allowed for the design of degenerate forward primers potentially able to target the entire molecular diversity of Ranidae AMPs. The reverse primer matched the poly-A tail of the mRNA. Amplicons resulting from cDNA PCR amplification were size selected and sequencing was carried out on an Ion PGM™ sequencing platform (Thermo Fisher Scientific, USA). Upon standard trimming procedure, reads were assembled into contigs with an overlap-layout-consensus (OLC) approach. Finally, AMP-encoding sequences were identified by similarity and virtually translated using the ExPASy translate tool [18].

Relatedness of the identified AMPs among themselves and with previously described anuran AMPs was carried out by a combination of BLASTn and multiple sequence alignment, principally concerning the nucleotide sequences of the propeptide and 3′UTR of the encoding mRNAs. These regions are relatively well conserved in AMPs and the identity can therefore be used to infer relatedness.

2.2. Peptide synthesis

Selected frog peptides were obtained from GenicBio Limited (Shanghai, China), all at > 98% purity and amidated at C-terminus, except Peptide-3 and -4, which had an acidic C-terminus and one disulphide bridge each. The correct structures were confirmed by RP-HPLC/MS (see Fig. S1). Chromatographic separation was achieved on a reversed-phase column (C18, 5 µm, 110 Å, 4.6 × 250 mm) using a 25–85% acetonitrile/0.1% TFA gradient in 25 min at a 1 mL/min flow rate. Peptide stock concentrations were determined by dissolving accurately weighed aliquots of peptide in doubly distilled water, and further verified by using the extinction coefficients at 214 nm, calculated as described by Kuipers and Gruppen [19].

2.3. Preparation of liposomes

LUVs (large unilamellar vesicles) were prepared by dissolving dry lipids, 1,2-dipalmitoyl-*sn*-phosphatidylglycerol (DPPG) and 1,2-dioleoyl-*sn*-glycero-3-phosphocholine (DOPC) (Avanti Polar Lipids, Alabaster, Alabama, USA) in chloroform/methanol (2:1) solution. The solution was evaporated using a dry nitrogen stream and vacuum-dried for 24 h. The dry lipid cake was resuspended in 1 mL of sodium phosphate buffer (SPB) to a concentration of 5 mM phospholipid and spun for 1 h at a temperature above the Tc (lipid critical temperature). The resulting multilamellar vesicle suspensions were disrupted by several freeze–thaw cycles before passing through a mini-extruder (Avanti Polar Lipids) successively using polycarbonate filters with 1 µm, 0.4 µm and 0.1 µm pores. The vesicles were resuspended to a final phospholipid concentration of 0.4 mM and 1 mM, for circular dichroism (CD) and surface plasmon resonance (SPR) experiments, respectively. Based on the bilayer membrane surface area of a ~100 nm diameter liposome, and the area of a phospholipid head group (~0.7–1 nm^2) [20] the concentration of liposomes is estimated at between 5 and 10 nM.

2.4. Circular dichroism

CD spectra were obtained on a J-710 spectropolarimeter (Jasco, Tokyo, Japan). The spectra are accumulations of three scans measured in *a*) SPB solution, *b*) 50% TFE in SPB, *c*) the presence of sodium dodecyl sulphate micelles (10 mM SDS in SPB), *d*) the presence of anionic LUVs (DPPG) in SPB or *e*) the presence of neutral LUVs (DOPC) in SPB. The helix content was determined as $[\theta]^{222}/[\theta]^{\alpha}$, where $[\theta]^{222}$ is the measured molar per/residue ellipticity at 222 nm under any given condition and $[\theta]^{\alpha}$ is the molar ellipticity for a perfectly formed alpha helix of the same length, estimated as described by Chen et al. [21].

2.5. Antibacterial activity

Minimal inhibitory concentration (MIC) was determined on four Gram-negative and Gram-positive laboratory strains from the American Type Culture Collection (ATCC, Rockville, MD, USA) including *E. coli* ATCC 25922, *Acinetobacter baumannii* ATCC 19606, *Staphylococcus aureus* ATCC 29213 and *Enterococcus faecalis* ATCC 29212 and multidrug resistant *S. aureus*. Its origin, antibiograms, and characterization of resistance determinants were described previously in Roncevic et al. [22]. Results were obtained using the serial two-fold microdilution method according to CLSI [23]. Bacteria were cultured in a fresh Mueller Hinton broth (MHB) (Biolife, Milano, Italy) or Enterococcus broth (BN Biosciences, Franklin Lakes, New Jersey, United States) to the

mid exponential phase, added to serial dilutions of synthetic peptides to a final load of 5×10^5 CFU/mL in 100 µL per well, and incubated at 37 °C for 18 h. MIC was visually determined as the lowest concentration of the peptide showing no detectable bacterial growth and it was a consensus value of an experiment performed in triplicate.

For determination of minimal bactericidal concentration (MBC), 4 µL of bacterial suspensions were taken from the wells corresponding to MIC, 2 × MIC, and 4 × MIC and then plated on MH or enterococci agar plates. Plates were incubated for 18 h at 37 °C to allow the viable colony counts and the MBC determined as the peptide concentration causing no visible growth.

2.6. Surface plasmon resonance

Interaction studies between selected peptides and model membranes were carried out on X100 instrument (Biacore, GE Life Sciences, Chicago, Illinois, United States) immobilizing integral liposomes on an L1 sensor chip surface [24]. DOPC liposomes were injected three times for 10 min with flow rate of 5 µL/min over the L1 sensor surface, until 9000 RU maximum was reached [25,26]. The binding of the peptides with the liposomes was determined injecting a peptide concentration series (0.5 to 32 µM) at 10 µL/min for a contact time of 540 s, followed by a dissociation time of 1200 s with PBS running buffer. Sensorgrams were obtained using BIAevaluation software v 1.1 (Biacore, GE Life Sciences) fitting the curves with the "Affinity - Steady State" mathematical model and then elaborated using GraphPad v 6.04 (GraphPad Software, La Jolla, California, USA). Each experiment was repeated two times.

2.7. Membrane integrity assay

The effect of the peptide-6 on bacterial membrane integrity was studied by measuring the percentage of propidium iodide (PI) positive cells after exposure to the peptide, using an Accuri C6 flow cytometer (BD Biosciences, CA, USA). Measurements were carried out on *S. aureus* ATCC 29213 cells which were cultured in MH medium to the mid logarithmic phase. After incubation, SYTO9/PI dye (LIVE/DEAD® BacLight™ Bacterial Viability Kits, Molecular Probes, Eugene, Oregon, USA) was added to the bacterial suspension (1×10^6 CFU/mL). Dye mixture was prepared and added to the suspension according to the manufacturer's instructions. Peptide was then added in concentrations corresponding to MIC, ½ MIC and ¼ MIC, just before the beginning of the analysis, and the measurement taken after 15, 30 and 60 min. Melittin was used as positive control, while stained untreated cells in MH medium were used as negative control. Non-stained cells and single stained samples were used to compensate fluorescence channels on the cytometer and adjust appropriate gates on dot-plots. Each measurement was conducted in triplicate, and for each incubation time at least 10,000 cells were collected. Data analysis was carried out with FlowLogic 6.0 software.

2.8. AFM images

S. aureus ATCC 29213 cells were investigated by AFM. Over-night culture growth, next-day dilutions and treatments were carried out as reported in Roncevic et al. [27]. Briefly, the bacteria were treated with 2 µM, 4 µM (corresponding to MIC and MBC) and 8 µM of the peptide-6 and incubated with shaking at 100 rpm at 37 °C for 1 h. The culture was then briefly centrifuged, and the pellet resuspended in one tenth of the supernatant. Melittin treated cells were prepared in the same way and treated with the peptide at 2 µM and 3.5 µM, corresponding to MIC and MBC respectively [28]. The control samples were prepared in the same fashion but without the peptide treatment. Bacterial adhesion to glass slides was enabled with Cell-Tak solution (Corning, NY, USA) coating [29] as reported in [27]. AFM measurements were carried out in contact mode, under ambient conditions, using Bruker Multimode 3 (Digital Instruments, USA) instrument with a 0.12 N/m silicon-nitride probe (Bruker AFM probes USA, DNPS-10). Scan rates during imaging were kept between 2 and 3 Hz, and the image resolution was 512 pixels per line. Analysis of the obtained images was carried out with Gwyddion.

2.9. Toxicity assay

The cytotoxic effect of peptides was determined initially on a human MEC-1 lymphoid tumor cell line [30]. Cells were cultured in RPMI 1640 medium supplemented with 2 mM L-glutamine, 100 U/mL penicillin, 100 µg/mL streptomycin, and 10% foetal bovine serum (FBS) (complete medium) and sub-cultured two–three times a week for maximum of 20 passages. Cells were counted by Trypan Blue exclusion test, diluted to 10^6 cells/mL and plated into 96-well culture plates. Cytotoxicity assays were also carried out on human monocytes and lymphocytes isolated from buffy coats of informed donors (in accordance with the ethical guidelines and approved from the ethical committee of the University of Trieste) [31]. Briefly, the buffy coats were diluted 1:1 with PBS and added to an equal volume of Histopaque-1077. After centrifugation for 30 min at 400 × *g*, the white band at the interphase between the plasma and the Histopaque fractions was recovered, transferred into a sterile tube and washed twice with PBS. The cell pellet was then resuspended in RPMI HEPES and transferred to a cell culture flask or multiwell plates. Monocytes were left to adhere for 90 min and then lymphocytes were recovered, as cells in suspension that were used within two days, maintaining them in RPMI 1640 medium supplemented with 2 mM L-glutamine, 100 U/mL penicillin, 100 µg/mL streptomycin and 10% foetal bovine serum (FBS) added with HEPES (25 mM), nEAA (1 mM), sodium pyruvate (1 mM), and 2ME (0.05 mM). Adherent monocytes, after gentle washing with warmed PBS, were cultured in complete medium and used within two days. The cells were incubated in humidified air with 5% CO_2 at 37 °C.

Metabolic activity was determined after treatment with the peptides in complete medium for 24 h. For this purpose, 20 µL of MTT dye (5 mg/mL) was added to each well (10^5 cells/well) and incubated for 4 h at 37 °C. Formazan crystals were solubilized with acidic isopropanol (0.04 N HCl in absolute isopropanol) and the absorbance measured at 540 nm and 630 nm with microplate reader (Tecan Sunrise, Männedorf, Switzerland). All measurements were done at least in triplicate.

In order to discriminate viable, late apoptotic and/or necrotic cells, flow cytometry measurements have been carried out on a Cytomics FC500 instrument (Beckman Coulter Inc., Fullerton, CA, USA), equipped with an argon laser (488 nm, 5 mV) and standard configuration. Prior to peptide treatments, cells were double stained with fluorescent probes, namely DiOC6 (3,3′-dihexyloxacarbocyanine iodide) (FluoProbes, Interchim, Montlucon Cedex, France) and PI. Briefly, DiOC6 was used as a marker of mitochondrial functionality and was incubated with the cells for 15 min at 37 °C (final concentration of 50 nM), washed twice with 2 mL of PBS and cells resuspended in PBS. Membrane integrity was assessed with PI which was added to DiOC6-stained cells at final concentration of 15 µM. Then, the cells were treated with peptides up to 60 min and measurement taken every 15 min. Cells treated with 50 µM of the uncoupler carbonyl cyanide 3-chlorophenylhydrazone (CCCP) at 37 °C for 15 min were run in parallel as positive control (collapse of mitochondrial transmembrane potential). Data analysis was performed with the FCS Express3 software (De Novo Software, Los Angeles, CA, USA). Data obtained from repeated experiments were subjected to computer-assisted analysis using GraphPad Instat 3, and statistical significance was assumed at $p \leq 0.05$ (ANOVA, Student-Newman-Keuls post-test).

Table 1
Ranidae peptide sequences and their physico-chemical characteristics.

Peptide	Coding sequence[a] [13]	Sequence[b]	Charge	H[c]
Peptide-1	rtemp_4.3_210	LVPFIGRTLGGLLARF-NH_2	+4	2.5
Peptide-2	rtemp_4.6_20	FLGALGNALSRVL-NH_2	+3	1.9
Peptide-3	rtemp_32_47	NNLRHIVAWCKNRNYSLAVCARFKPQ	+6	−1.6
Peptide-4	rdal_39_24	NLLGFLQGAKDILKECEADNYQGWLCESYKPQ	−1	−1.3
Peptide-5	rdal_8_600	FLGFVGQALNALLGKL-NH_2	+3	2.5
Peptide-6	rarv_10.1_19	LLGAALSALSSVIPSVISWFQK-NH_2	+3	1.9

[a] Peptide name consists of the first letter of the frog genus where the peptide was identified, followed by 3 or 4 letters pertaining to the species name. First number refers to the contig where the peptide was found, and the second one to the number of reads supporting it.
[b] All amidated sequences end with a C-terminal amidation signal (-GK, -GKR) [34,35].
[c] Calculated using the CCS consensus hydrophobicity scale [33].

3. Results and discussion

3.1. Novel peptide sequences

Selective amplification with AMP specific primers of cDNA libraries obtained from five Ranidae species allowed for high-throughput, parallel identification of 127 peptides. Out of those, 29 sequences had either no identity, < 80% identity or 100% identity but with < 70% query cover, with known protein sequences when searched by BLAST [32] against the non-redundant protein database (described in detail in Roncevic et al. [13]). Six peptides were selected for chemical synthesis and activity verification. These peptides were selected on the basis of their different charge (from −1 to +6), hydrophobicity (from −1.6 to 2.5 calculated using the CCS consensus hydrophobicity scale [33]), structural aspects (likely helical conformation or presence of a disulphide bridge) and/or amidated C-terminus (see Table 1). Peptide-3 and -4 contain two Cys residues which likely result in the formation of a disulphide bridge. All other peptides are linear and most likely adopt a helical conformation to some extent.

3.2. Comparison to previously characterized anuran AMPs

As previously reported [13], the six peptides selected for synthesis were chosen based on both molecular diversity and sequence novelty, i.e. the lack of detectable similarity of the mature peptide region with previously characterized anuran AMPs. However, the detailed investigation of the propeptide and 3′UTR regions of the encoding mRNAs might provide meaningful information concerning the evolutionary origins of these sequences. Indeed, both regions are expected to be subject to purifying selection due to their regulatory roles in AMP processing/maturation and post-translational regulation [36–38].

From an evolutionary perspective, peptide-1 and -2 from *R. temporaria* appear to be closely related to previously characterized temporins, including temporin-A (rtemp_1.10_80), -B (rtemp_1_852), -C (rtemp_2_141) -F (rtemp_107_11), -L (rtemp_4.21_24), (the codes indicate that these known sequences were among the ones revealed by our DNA sampling method, see Roncevic et al. [13]), as well as to the novel AMP sequence rtemp_4.7_33. Two of the newly synthesized peptides (peptides-1 and -2, corresponding to rtemp_4.3_210 and rtemp_4.6_20) share significant homology with known temporins, in particular in the propeptide region (100% and 92.78% identity with temporin-A, respectively), and in the 3′UTR regions (96.70% and 86.32% identity with temporin-F and -L, respectively) (see Table S1). Moreover, the length of the mature peptide region of rtemp_4.6_20, including the C-terminal –GK amidation signal, is identical to that of all other temporins (15 amino acids), whereas the slightly superior length of rtemp_4.3_210 can be linked to the presence of a 9 residue insertion within the ORF. Altogether, these data suggest a relatively recent origin of the two novel peptides from the duplication of a temporin gene, followed by rapid diversification of the mature peptide region by positive selection.

On the other hand, while peptide-3 from the same species (rtemp_32_47) does not conform to any cluster of paralogous sequences, it shows significant similarity with rdal_39_24 from *R. dalmatina*, another of the peptides selected for synthesis (peptide-4). Indeed, the two sequences score reciprocal best BLAST hits in inter-species comparisons, due to the presence of highly conserved sequence stretches in the propeptide (77 identical nucleotides out of 80) and 3′UTR (46 identical nucleotides out of 50) regions, which suggest that the two sequences are orthologous. In spite of the presence of multiple indels within the ORF in the mature peptide region, both sequences are characterized by the presence of two cysteine residues and by an unusual KPQ C-terminal motif. Curiously, no other potential orthologous (nor paralogous) sequence could be identified in any of the other target anuran species, including the congeneric *R. arvalis*.

The fifth peptide selected for de novo synthesis, rdal_8_600 from *R. dalmatina*, also appears to be related to temporins, due to a high level of identity with rdal_21_605 (temporin-F) and rdal_40_14 (also belonging to the temporin sequence cluster). Compared to these two sequences, rdal_8_600 displays a 9 nucleotide long insertion within the mature peptide region, maintains the C-terminal –GK amidation signal and shows a 93.5% identical 3′UTR. No clear orthologous AMP sequence could be detected in any of the other target Ranidae species.

Peptide-6 (rarv_10.1_19) from *R. arvalis*, does not conform to any known AMP family and, at the same time, appears to be present as a single-copy gene in all *Rana* species. Sequences clearly orthologous to peptide-6 could in fact be retrieved with our approach in *R. temporaria* (rtemp_88_19 – FIGSALKVLAGVLPSVISWVKQG, processed sequence - FIGSALKVLAGVLPSVISWVKQ-NH_2) and *R. dalmatina* (partial sequence, possibly due to a poor expression level). Rtemp_88_19 was initially discarded [13] discarded due to a poor support by sequencing data. It shares the same length and 74% sequence identity with peptide-6 at the amino acid level.

3.3. Peptide structure

The CD spectra of all six peptides were measured under different conditions, including aqueous buffer, anionic SDS micelles, 50% trifluoroethanol and anionic (DPPG) or neutral zwitterionic (DOPC) LUVs. All peptides are substantially disordered in an aqueous environment, although peptides-3 and -4 show some structuring, likely due to the presence of a disulphide bridge (see Fig. 1). Peptide-1 showed a marked conformational change in the presence of TFE to a spectrum typical for an α-helix. The transition is less marked in the presence of SDS or of neutral LUVs, but quite as marked in the presence of anionic LUVs, although the shape is different (see Fig. 1 and Table S2). We have previously explained the dominance of a minimum at 225 nm with respect to 208 as being due either to self-aggregation at the membrane surface or to the adoption of a 3–10 type helical conformation [27]. In any case it suggests a selective interaction with anionic membrane surfaces. Peptide-2 instead behaves as a canonical helical peptide under all conditions except aqueous, and again the effect is strongest in the

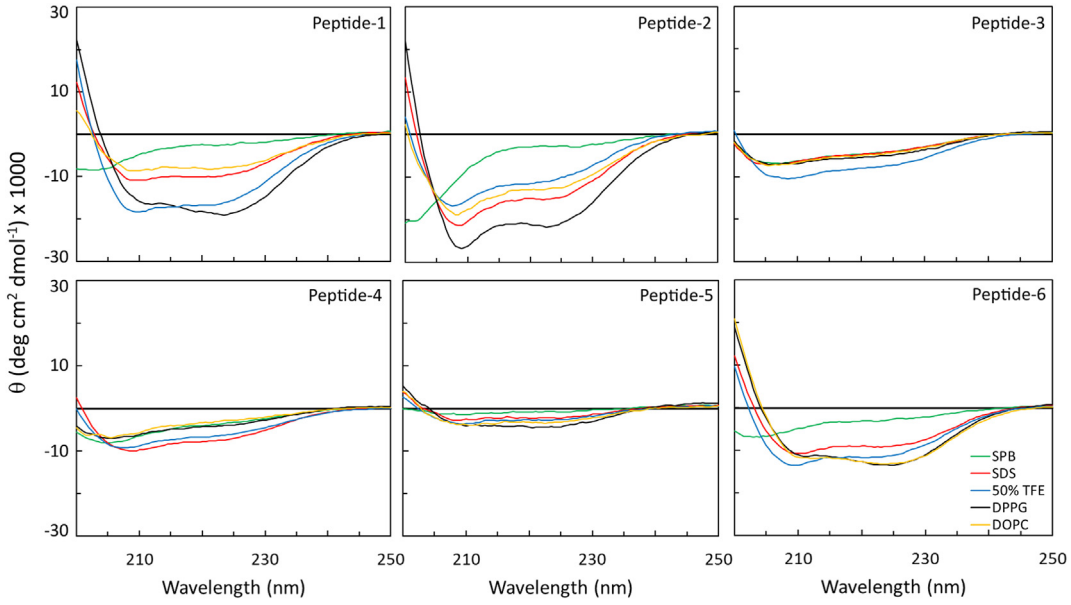

Fig. 1. CD spectra of frog peptides under different conditions. Spectra are the accumulation of three scans carried out with 20 μM peptide in SPB, 10 mM SDS in SPB, 50% TFE, anionic LUVs in SPB (DPPG, 5 nM) and neutral LUVs in SPB (DOPC, 5 nM).

presence of DOPC LUVS, suggesting it inserts into these membranes as a lone α-helix (see Fig. 1 and Table S2). Peptides-3 and -4 show the least change in conformation, which may indicate that they do not interact strongly with a membrane like environment, or that the interaction does not markedly affect their conformation. Note that while a lack of interaction would not be surprising for peptide-4 with DPPG LUVs, as it is anionic, for peptide-3 which is strongly cationic interaction with the surface of DPPG LUVs is to be expected. Peptide-5 shows rather weak spectra but it substantially follows the same trend as peptide-1. Peptide-6 instead differentiates from peptide-1 in that the spectra are very similar in the presence of DPPG or DOPC LUVs, again showing a minimum at 225 nm (see Fig. 1 and Table S2). This would suggest that peptide-1 could be more selective of bacterial membranes with respect to host cell membranes than peptide-6.

3.4. Antibacterial activity

The antibacterial activity of Ranidae peptides was assessed against four reference bacterial strains and one clinical isolate. Out of the six tested peptides, only peptide-6 showed appreciable antibacterial potential (see Table 2) with a certain selectivity towards Gram-positive bacteria, especially *S. aureus* (MIC = MBC = 4 μM). The activity was also tested against a multi-drug resistant isolate of *S. aureus*, with only moderately increased MIC and MBC (8 and 16 μM, respectively). Peptide-6 also showed a moderate activity against *E. faecalis* (MIC and MBC = 16 μM). Out of the remaining five peptides, peptide-1, -2 and -5 showed some activity against *S. aureus* with MIC values ranging from 16 to 32 μM (see Table 2). It should however be noted that when tested in reduced medium (20% MH), MIC values decreased several-fold for all the above peptides (see Table S3) suggesting that antimicrobial activity is rather medium/salt sensitive. This is, in fact, rather common for antimicrobial peptides and is one of the reasons why clinical trials are mostly limited to topical applications (e.g. pexiganan for treatment of impetigo and diabetic ulcers) [5]. Peptide-3 and -4 were inactive, irrespective of the medium conditions used, so they may not be conventional AMPs but have other biological functions [39], or the bacterial susceptibility to these AMPs may be significantly higher in the particular ionic environment in the physical district where they are produced, analogously to previously reported examples for mammalian AMPs [40].

3.5. Model membrane interaction

Interaction with the DOPC membrane was evaluated on peptide-1 and -6. The binding sensorgrams indicate that both peptides are able to bind a model membrane, since the binding response units (RU) increased with the peptide concentrations (see Fig. 2), but the interaction seems to be somewhat different. During the dissociation phase, the binding curve for peptide-1, at 32 μM, does not return to the baseline after washing with PBS, indicating the formation of stable and irreversible complex with the membrane (see Fig. 2 a)). The binding curve does not reach saturation binding so the K_D value was only approximately estimated to be 5×10^{-4} M (see Fig. 2 b)). For peptide-6, binding increased sharply and non-linearly with concentration, with a significant jump in the signal at 16 μM, suggesting self-aggregation and/or oligomerization on the liposome surface [41] (see Fig. 2 c) and

Table 2
Antibacterial activity (μM) of Ranidae peptides against Gram-negative and Gram-positive bacterial strains in MH medium.

Bacterial strains	Peptide-1		Peptide-2		Peptide-3		Peptide-4		Peptide-5		Peptide-6	
	MIC	MBC	MIC	MBC	MIC	MBC	MIC	MBC	MIC	MBC	MIC	MBC
S. aureus ATCC 29213	16	16	32	64	> 64	/	> 64		32	32	4	4
S. aureus c.i.	64	64	NA[a]	NA	NA	NA	NA	NA	NA	NA	8	16
E. faecalis ATCC 29212	> 64	/	> 64	/	> 64	/	NA		> 64	/	16	16
E. coli ATCC 25922	> 64	/	> 64	> 64	> 64	/	> 64		> 64	/	> 64	/
A. baumannii ATCC 19606	> 64	/	> 64	/	> 64	/	NA		> 64	/	32	64

[a] NA = not available.

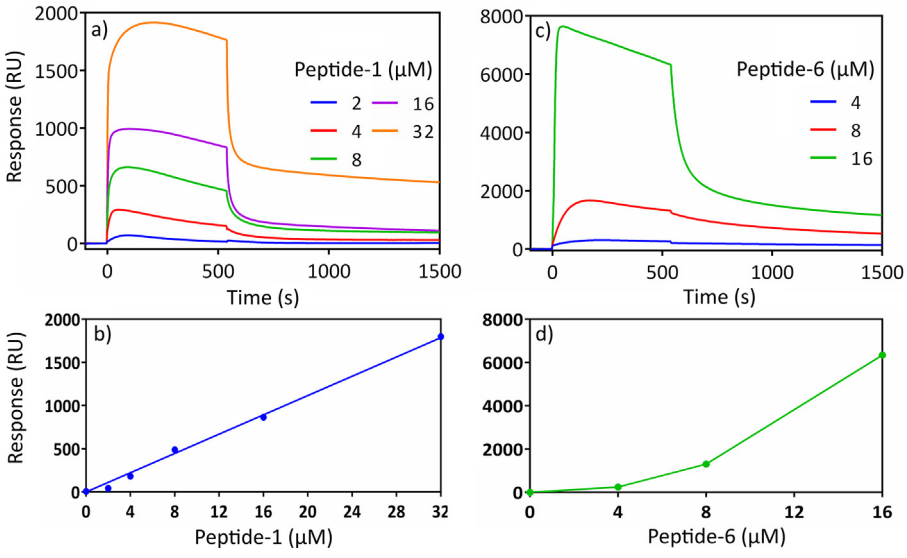

Fig. 2. Binding sensorgrams (top) and binding curves (bottom) for peptide-1 (A–B) and peptide-6 (C–D). Sensorgrams were obtained by applying peptides at increasing concentrations over DOPC LUVs immobilized on a L1 sensor chip. Binding curves were fitted using the "Affinity-Steady State" mathematical model. Shown is one experiment out of two different evaluations with very similar results.

d)). These effects make it difficult to estimate a proper "binding curve" for peptide-6 so that it was not possible to calculate the K_D value.

These results are in agreement with CD spectra, where self-aggregation/oligomerization is indicated by the $\theta^{208}/\theta^{222}$ ratio and were observed for peptide-6 in the presence of both DPPG model membrane (mimicking the anionic bacterial membrane), and DOPC LUVs (mimicking neutral host cell membrane). Interaction and self-aggregation/oligomerization in the presence of the different types of membranes may be related to antimicrobial (see Table 2) and cytotoxic effects on host cells (see below).

3.6. Effect on bacterial membrane integrity

Peptide-6 was further evaluated for its effect on the *S. aureus* membrane integrity, as the peptide was most active against this particular strain (see Table 2). AFM imaging was used to visualize cell wall damage, while flow cytometry was used to monitor PI uptake. Significant PI uptake is often observed for other α-helical peptides, that tend to be membranolytic [42]. Treatment of bacterial cells with peptide-6 caused only slight membrane permeability at sub-MIC concentrations, with < 20% PI+ cells after 1 h incubation (see Fig. 3). The effect is somewhat more pronounced at MIC (4 μM), and is time dependent, with PI+ cells increasing to ~40% after 60 min exposure (see Fig. 3).

The effect of peptide-6 on *S. aureus* cell wall was also investigated by AFM, as compared to untreated cells. The latter showed a smooth cell wall surface without visible perturbations or disruptions. Cells have a characteristic cocci shape and remain attached post division (see Fig. 4 a)). After treatment with peptide-6 at sub-MIC concentration (2 μM), the cell morphology did not change to a significant extent (see Fig. 4 d)), while treatment at 4 μM resulted in significant cellular damage for some of the cells while some remained relatively undisturbed (see Fig. 4 e)). This effect is mostly pronounced at 2 × MIC (8 μM) as all cells are ruptured and their morphology is altered (see Fig. 4 f)). It is interesting to note that cell wall damage is less evident for the cells treated with the known membranolytic peptide melittin at its MIC (2 μM) and MBC (3.5 μM) (see Fig. 4 b) and c)). On the other hand, the PI-uptake assay suggests melittin has a strong membranolytic effect causing ~100% permeability after only 15 min incubation (see Fig. 3), which is consistent with previous reports [43–45]. It is evident both peptides are active against *S. aureus* at similar concentrations but apparently with somewhat different modes of action. In the case of peptide-6 this may include self-aggregation/oligomerization as suggested by SPR assay and CD spectra (see above), which may play a role in membrane perturbation, as reported for membrane translocation peptides [46].

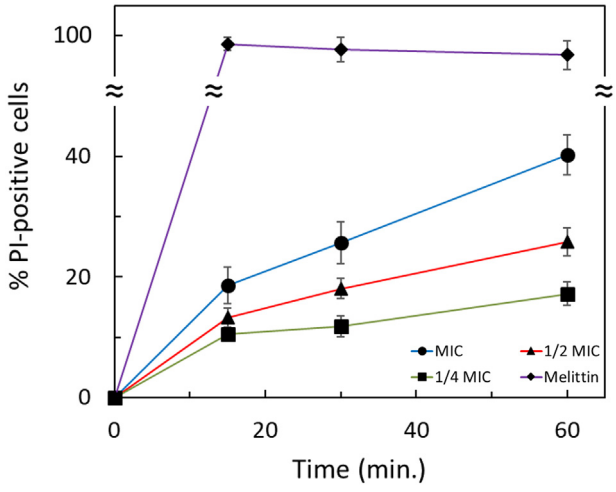

Fig. 3. Evaluation of the effect of peptide-6 on bacterial membrane integrity. Peptide was incubated with *S. aureus* ATCC 29213 (1×10^6 CFU/mL) for 60 min at concentrations equal to ¼ MIC, ½ MIC and MIC. Melittin was used as positive control at 5 μM. Data are expressed as the mean of % PI positive cells ± SEM of three independent experiments.

3.7. Cytotoxic effects

Both of the most active peptides (-1 and -6) were tested for their cytotoxic effects on different types of cells. Results on the MEC-1 cell line indicate that peptide-6 is somewhat more toxic than peptide-1. This is especially evident at > 50 μM concentration (see Fig. 5), although the IC_{50} value (44 μM) is significantly higher than the anti-*S. aureus*. Peptide-1 has a lower tendency to damage these cells with IC_{50} value at 105 μM (see Fig. 5). Both peptides were also examined for their mechanism of action to induce cell damage at concentrations ranging from 10 to 25 μM (MIC-MBC range). Dot-plots of the double stained cells show that MEC-1 cells are sensitive to apoptotic damage induced only by peptide-6, in a concentration-dependent manner (~40% and < 20% viable cells, respectively, at 10 and 25 μM, see Fig. S2, panels D–F). For comparison, peptide-1 (which showed a low but detectable cytotoxicity in the MTT assay), under the same conditions resulted in ~90% viable cells (see Fig. S2, panels B and C), comparable to untreated controls (see

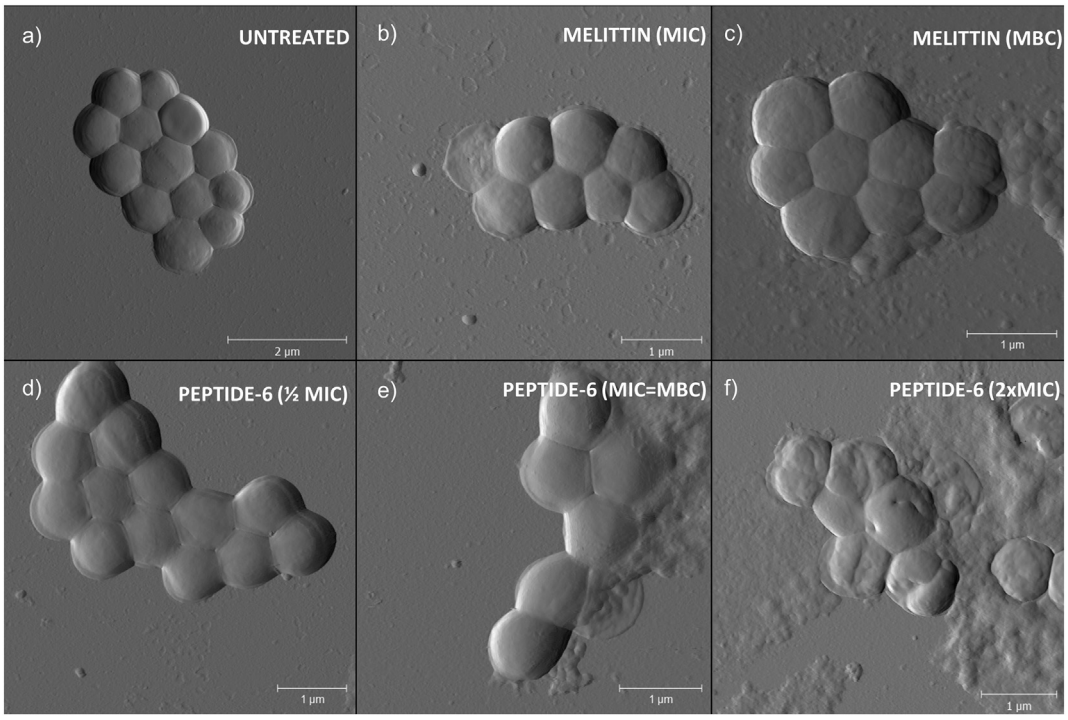

Fig. 4. AFM deflection (error) images of *S. aureus* ATCC 29213 cells. Bacteria were exposed to the peptide-6 at concentrations equivalent to the ½ MIC, MIC (MBC) and 2 × MIC.

Fig. S2, panel A, LR quadrant). Other peptides were not tested as they were found to be nontoxic in the MTT assay (see Fig. S3).

Although commonly used for studying cytotoxic effects [47], the MEC-1 cell line is in fact derived from tumor cells (B-chronic lymphocytic leukemia [30]). Neoplastic cells have features such as a more anionic membrane [48], that were previously correlated with enhanced peptides' tendency to interact with and disrupt cell membrane [49]. For this reason, the peptides' ability to induce cytotoxic effects was also tested on PBMC (resting circulating monocytes and lymphocytes derived from healthy donors) and for both peptide-1 and -6, the highest concentrations tested (100 µM) resulted in a cell viability > 80% (see Fig. 6). Based on these results, peptide-6 may be less toxic to normal than cancer-derived cells.

4. Conclusions

Six novel secretion peptides, derived from a targeted sequencing approach carried out simultaneously on five Ranidae species, were synthesized and one, identified from *R. arvalis*, showed significant activity against *S. aureus*, including a multi-drug resistant clinical isolate. This peptide appears to disrupt the bacterial membrane active concentrations and alters cell morphology at concentrations corresponding to 2 × MIC. Its activity is comparable to that of melittin, a potent membranolytic peptide derived from bee venom, but with somewhat different mechanism. Its mode-of-action may include self-aggregation/oligomerization at the membrane surface, which may be an initial step for membrane perturbation. The peptide toxicity against human circulating blood cells is negligible, with > 80% viable cells when tested at 100 µM concentration (considerably higher than to MIC value). It is somewhat more toxic against leukemia derived MEC-1 cells even

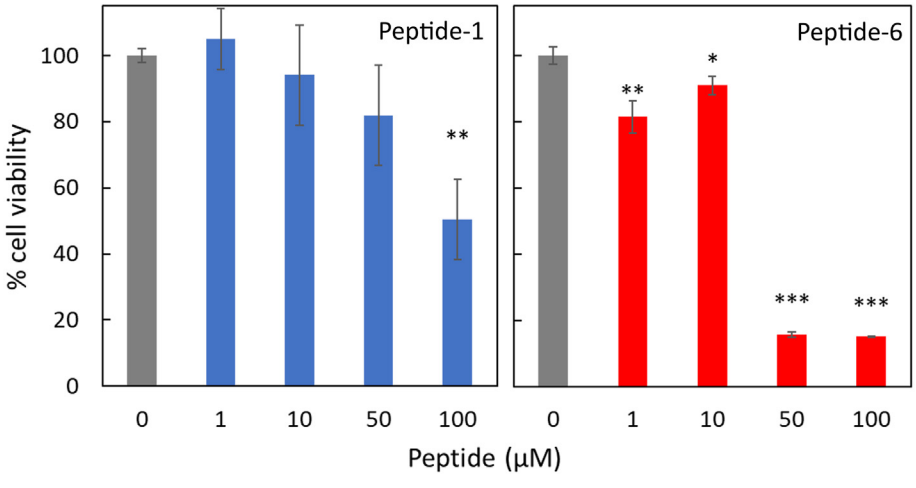

Fig. 5. Evaluation of cell viability in MEC-1 cells after exposure to peptide-1 and -6. Cells were exposed to 1, 10, 50, and 100 µM peptide for 24 h and evaluated by MTT assay. Viability is presented as % of the corresponding controls (*$p < 0.05$, **$p < 0.01$, ***$p < 0.001$).

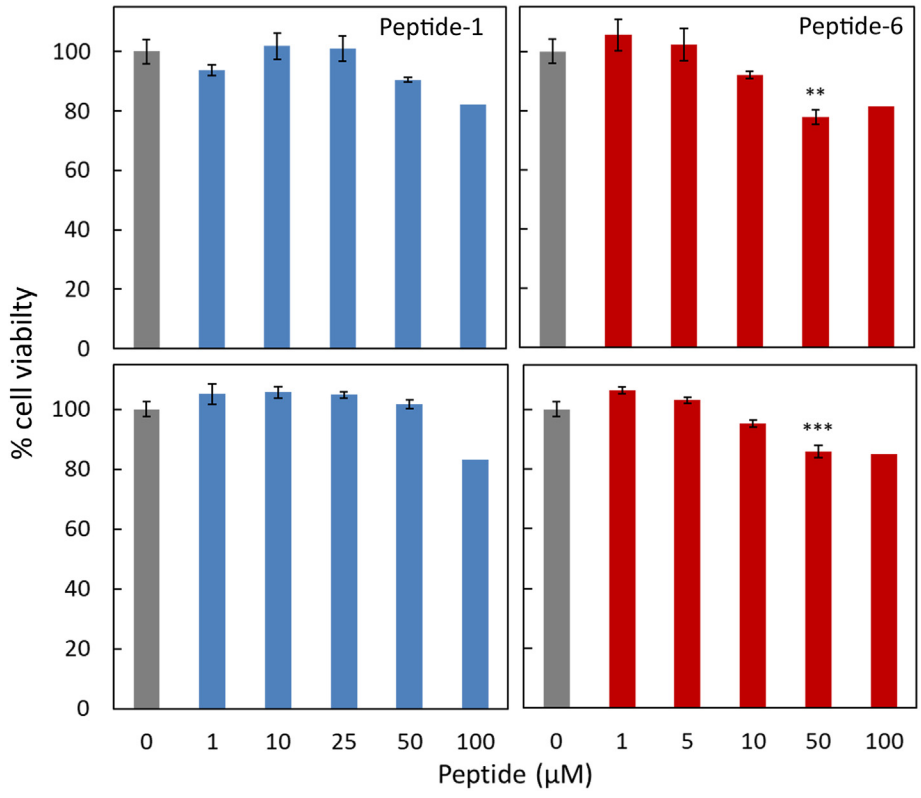

Fig. 6. Evaluation of cell viability in monocytes (lower panel) and lymphocytes (upper panel) after exposure to peptide-1 and -6. Cells were exposed to peptides up to 100 μM for 24 h and evaluated by MTT assay. Viability is presented as % of the corresponding controls (*$p < 0.05$, **$p < 0.01$, ***$p < 0.001$).

though the IC_{50} value remains several-fold higher compared to its MIC against *S. aureus*. In terms of possible biomedical application, the results are promising and suggest peptide-6 has a good selectivity for *S. aureus*, causing little damage to host cells at concentrations several-fold higher than the MIC values. All other peptides were only moderately or weakly active against bacteria, under the conditions used, in a salt/medium sensitive manner, and in general selective for Gram-positive strains.

It may thus be useful, in future analyses, to further study the effect of medium conditions on antimicrobial activity. Furthermore, as the activity did not correlate directly with membrane interactions (as assessed by CD), it may be useful to determine how membrane composition could affect activity. It may also be revealing to expand the tested bacteria, possibly including ones that tend to infect the host species, for possible narrow selectivity. It cannot however be excluded that the peptides have defense activities not involving direct bacterial inactivation.

Phylogenetic investigations revealed that peptide-6 does not pertain to any of the previously characterized anuran AMP families and is likely present as a single-copy gene in multiple species within the *Rana* genus. In the light of its appreciable antimicrobial activity, future investigations could be directed towards an orthologous AMP sequence identified in *R. temporaria*.

CRediT authorship contribution statement

Tomislav Rončević: Conceptualization, Methodology, Formal analysis, Investigation, Writing - original draft, Writing - review & editing, Visualization. **Lucija Krce:** Methodology, Investigation, Formal analysis, Visualization. **Marco Gerdol:** Formal analysis, Investigation. **Sabrina Pacor:** Investigation. **Monica Benincasa:** Investigation. **Filomena Guida:** Investigation. **Ivica Aviani:** Methodology, Formal analysis. **Vedrana Čikeš-Čulić:** Methodology, Investigation. **Alberto Pallavicini:** Methodology, Formal analysis. **Ana Maravić:** Investigation. **Alessandro Tossi:** Methodology, Formal analysis, Writing - original draft, Writing - review & editing, Supervision.

Acknowledgments

The authors acknowledge funding from Croatian Science Foundation [grant number 8481], Student Quorum University of Split (No. 2181-202-01-01-17-0028) and Erasmus+ (No. 2181-202-02-07-17-0149). The authors would also like to thank Francesca Grazioli from Department of Life Sciences, University of Trieste for her kind assistance with in vitro testing and the Laboratory for Clinical Microbiology at the University Hospital Centre Split, Croatia for providing clinical bacterial isolate used in the study. The authors also thank Dr. Luisa Lundin from BD Biosciences for her valuable assistance in setting up bacterial membrane permeabilization protocol.

References

[1] A. Nijnik, R. Hancock, Host defence peptides: antimicrobial and

immunomodulatory activity and potential applications for tackling antibiotic-resistant infections, Emerg. Health Threats J. 2 (2009), https://doi.org/10.3134/ehtj.09.001.
[2] A. Cederlund, G.H. Gudmundsson, B. Agerberth, Antimicrobial peptides important in innate immunity: antimicrobial peptides important in innate immunity, FEBS J. 278 (2011) 3942–3951, https://doi.org/10.1111/j.1742-4658.2011.08302.x.
[3] E. Tacconelli, Global Priority List of Antibiotic-resistant Bacteria to Guide Research, Discovery, and Development of New Antibiotics, (2017).
[4] M. Mahlapuu, J. Håkansson, L. Ringstad, C. Björn, Antimicrobial peptides: an emerging category of therapeutic agents, Front. Cell. Infect. Microbiol. 6 (2016), https://doi.org/10.3389/fcimb.2016.00194.
[5] S.-J. Kang, S.J. Park, T. Mishig-Ochir, B.-J. Lee, Antimicrobial peptides: therapeutic potentials, Expert Rev. Anti-Infect. Ther. 12 (2014) 1477–1486, https://doi.org/10.1586/14787210.2014.976613.
[6] K. Fosgerau, T. Hoffmann, Peptide therapeutics: current status and future directions, Drug Discov. Today 20 (2015) 122–128, https://doi.org/10.1016/j.drudis.2014.10.003.
[7] D.L. Paterson, P.N.A. Harris, Colistin resistance: a major breach in our last line of defence, Lancet Infect. Dis. 16 (2016) 132–133, https://doi.org/10.1016/S1473-3099(15)00463-6.
[8] Y.-Y. Liu, Y. Wang, T.R. Walsh, L.-X. Yi, R. Zhang, J. Spencer, Y. Doi, G. Tian, B. Dong, X. Huang, L.-F. Yu, D. Gu, H. Ren, X. Chen, L. Lv, D. He, H. Zhou, Z. Liang, J.-H. Liu, J. Shen, Emergence of plasmid-mediated colistin resistance mechanism MCR-1 in animals and human beings in China: a microbiological and molecular biological study, Lancet Infect. Dis. 16 (2016) 161–168, https://doi.org/10.1016/S1473-3099(15)00424-7.
[9] L. Fan, J. Sun, M. Zhou, J. Zhou, X. Lao, H. Zheng, H. Xu, DRAMP: a comprehensive data repository of antimicrobial peptides, Sci. Rep. 6 (2016) 24482, , https://doi.org/10.1038/srep24482.
[10] A. Ladram, Antimicrobial peptides from frog skin biodiversity and therapeutic promises, Front. Biosci. 21 (2016) 1341–1371, https://doi.org/10.2741/4461.
[11] M. Zasloff, Magainins, a class of antimicrobial peptides from *Xenopus* skin: isolation, characterization of two active forms, and partial cDNA sequence of a precursor, Proc. Natl. Acad. Sci. U. S. A. 84 (1987) 5449–5453.
[12] J.M. Conlon, J. Kolodziejek, N. Nowotny, Antimicrobial peptides from ranid frogs: taxonomic and phylogenetic markers and a potential source of new therapeutic agents, Biochim. Biophys. Acta BBA Proteins Proteomics 1696 (2004) 1–14, https://doi.org/10.1016/j.bbapap.2003.09.004.
[13] T. Rončević, M. Gerdol, F. Spazzali, F. Florian, S. Mekinić, A. Tossi, A. Pallavicini, Parallel identification of novel antimicrobial peptide sequences from multiple anuran species by targeted DNA sequencing, BMC Genomics 19 (2018), https://doi.org/10.1186/s12864-018-5225-5.
[14] A. Giuliani, A.C. Rinaldi (Eds.), Antimicrobial Peptides, Humana Press, Totowa, NJ, 2010, http://link.springer.com/10.1007/978-1-60761-594-1 , Accessed date: 12 December 2016.
[15] S.N. Stuart, J.S. Chanson, N.A. Cox, B.E. Young, A.S.L. Rodrigues, D.L. Fischman, R.W. Waller, Status and trends of amphibian declines and extinctions worldwide, Science 306 (2004) 1783–1786, https://doi.org/10.1126/science.1103538.
[16] M. Novkovic, J. Simunic, V. Bojovic, A. Tossi, D. Juretic, DADP: the database of anuran defense peptides, Bioinformatics 28 (2012) 1406–1407, https://doi.org/10.1093/bioinformatics/bts141.
[17] Y. Kodama, M. Shumway, R. Leinonen, The sequence read archive: explosive growth of sequencing data, Nucleic Acids Res. 40 (2012) D54–D56, https://doi.org/10.1093/nar/gkr854.
[18] E. Gasteiger, A. Gattiker, C. Hoogland, I. Ivanyi, R.D. Appel, A. Bairoch, ExPASy: the proteomics server for in-depth protein knowledge and analysis, Nucleic Acids Res. 31 (2003) 3784–3788.
[19] B.J.H. Kuipers, H. Gruppen, Prediction of molar extinction coefficients of proteins and peptides using UV absorption of the constituent amino acids at 214 nm to enable quantitative reverse phase high-performance liquid chromatography–mass spectrometry analysis, J. Agric. Food Chem. 55 (2007) 5445–5451, https://doi.org/10.1021/jf070337l.
[20] A. Tossi, L. Sandri, A. Giangaspero, Amphipathic, α-helical antimicrobial peptides, Pept. Sci. 55 (2000) 4–30.
[21] Y.-H. Chen, J.T. Yang, K.H. Chau, Determination of the helix and β form of proteins in aqueous solution by circular dichroism, Biochemistry (Mosc) 13 (1974) 3350–3359.
[22] T. Rončević, G. Gajski, N. Ilić, I. Goić-Barišić, M. Tonkić, L. Zoranić, J. Simunić, M. Benincasa, M. Mijaković, A. Tossi, D. Juretić, PGLa-H tandem-repeat peptides active against multidrug resistant clinical bacterial isolates, Biochim. Biophys. Acta BBA Biomembr. 1859 (2017) 228–237, https://doi.org/10.1016/j.bbamem.2016.11.011.
[23] Clinical and Laboratory Standards Institute, Performance Standards for Antimicrobial Susceptibility Testing, (2017).
[24] G. Anderluh, M. Beseničar, A. Kladnik, J.H. Lakey, P. Maček, Properties of nonfused liposomes immobilized on an L1 Biacore chip and their permeabilization by a eukaryotic pore-forming toxin, Anal. Biochem. 344 (2005) 43–52, https://doi.org/10.1016/j.ab.2005.06.013.
[25] E. Danelian, A. Karlén, R. Karlsson, S. Winiwarter, A. Hansson, S. Löfås, H. Lennernäs, M.D. Hämäläinen, SPR biosensor studies of the direct interaction between 27 drugs and a liposome surface: correlation with fraction absorbed in humans, J. Med. Chem. 43 (2000) 2083–2086, https://doi.org/10.1021/jm991156g.
[26] C.L. Baird, E.S. Courtenay, D.G. Myszka, Surface plasmon resonance characterization of drug/liposome interactions, Anal. Biochem. 310 (2002) 93–99, https://doi.org/10.1016/S0003-2697(02)00278-6.
[27] T. Rončević, D. Vukičević, N. Ilić, L. Krce, G. Gajski, M. Tonkić, I. Goić-Barišić, L. Zoranić, Y. Sonavane, M. Benincasa, D. Juretić, A. Maravić, A. Tossi, Antibacterial activity affected by the conformational flexibility in glycine–lysine based α-helical antimicrobial peptides, J. Med. Chem. 61 (2018) 2924–2936, https://doi.org/10.1021/acs.jmedchem.7b01831.
[28] I. AL-Ani, S. Zimmermann, J. Reichling, M. Wink, Pharmacological synergism of bee venom and melittin with antibiotics and plant secondary metabolites against multidrug resistant microbial pathogens, Phytomedicine 22 (2015) 245–255, https://doi.org/10.1016/j.phymed.2014.11.019.
[29] R. Louise Meyer, X. Zhou, L. Tang, A. Arpanaei, P. Kingshott, F. Besenbacher, Immobilisation of living bacteria for AFM imaging under physiological conditions, Ultramicroscopy 110 (2010) 1349–1357, https://doi.org/10.1016/j.ultramic.2010.06.010.
[30] A. Stacchini, M. Aragno, A. Vallario, A. Alfarano, P. Circosta, D. Gottardi, A. Faldella, G. Rege-Cambrin, U. Thunberg, K. Nilsson, MEC1 and MEC2: two new cell lines derived from B-chronic lymphocytic leukaemia in prolymphocytoid transformation, Leuk. Res. 23 (1999) 127–136.
[31] C. Pelillo, M. Benincasa, M. Scocchi, R. Gennaro, A. Tossi, S. Pacor, Cellular internalization and cytotoxicity of the antimicrobial proline-rich peptide Bac7(1-35) in monocytes/macrophages, and its activity against phagocytosed Salmonella typhimurium, Protein Pept. Lett. 21 (2014) 382–390.
[32] S.F. Altschul, T.L. Madden, A.A. Schäffer, J. Zhang, Z. Zhang, W. Miller, D.J. Lipman, Gapped BLAST and PSI-BLAST: a new generation of protein database search programs, Nucleic Acids Res. 25 (1997) 3389–3402.
[33] A. Tossi, L. Sandri, A. Giangaspero, New consensus hydrophobicity scale extended to non-proteinogenic amino acids, Peptides 27 (2002) 416.
[34] M.L. Mangoni, Y. Shai, Temporins and their synergism against Gram-negative bacteria and in lipopolysaccharide detoxification, Biochim. Biophys. Acta BBA Biomembr. 1788 (2009) 1610–1619, https://doi.org/10.1016/j.bbamem.2009.04.021.
[35] R.G. Solstad, C. Li, J. Isaksson, J. Johansen, J. Svenson, K. Stensvåg, T. Haug, Novel antimicrobial peptides EeCentrocins 1, 2 and EeStrongylocin 2 from the edible sea urchin *Echinus esculentus* have 6-Br-Trp post-translational modifications, PLoS One 11 (2016) e0151820, , https://doi.org/10.1371/journal.pone.0151820.
[36] M. Zasloff, Antimicrobial peptides of multicellular organisms, Nature 415 (2002) 389–395, https://doi.org/10.1038/415389a.
[37] Y. Gao, D. Wu, X. Xi, Y. Wu, C. Ma, M. Zhou, L. Wang, M. Yang, T. Chen, C. Shaw, Identification and characterisation of the antimicrobial peptide, phylloseptin-PT, from the skin secretion of *Phyllomedusa tarsius*, and comparison of activity with designed, cationicity-enhanced analogues and diastereomers, Molecules 21 (2016) 1667, https://doi.org/10.3390/molecules21121667.
[38] M. Zanetti, R. Gennaro, D. Romeo, Cathelicidins: a novel protein family with a common proregion and a variable C-terminal antimicrobial domain, FEBS Lett. 374 (1995) 1–5, https://doi.org/10.1016/0014-5793(95)01050-O.
[39] Y. Lai, R.L. Gallo, AMPed up immunity: how antimicrobial peptides have multiple roles in immune defense, Trends Immunol. 30 (2009) 131–141, https://doi.org/10.1016/j.it.2008.12.003.
[40] R.A. Dorschner, B. Lopez-Garcia, A. Peschel, D. Kraus, K. Morikawa, V. Nizet, R.L. Gallo, The mammalian ionic environment dictates microbial susceptibility to antimicrobial defense peptides, FASEB J. 20 (2006) 35–42, https://doi.org/10.1096/fj.05-4406com.
[41] D. Xhindoli, F. Morgera, U. Zinth, R. Rizzo, S. Pacor, A. Tossi, New aspects of the structure and mode of action of the human cathelicidin LL-37 revealed by the intrinsic probe p-cyanophenylalanine, Biochem. J. 465 (2015) 443–457, https://doi.org/10.1042/BJ20141016.
[42] H. Sato, J.B. Feix, Peptide–membrane interactions and mechanisms of membrane destruction by amphipathic α-helical antimicrobial peptides, Biochim. Biophys. Acta BBA Biomembr. 1758 (2006) 1245–1256, https://doi.org/10.1016/j.bbamem.2006.02.021.
[43] G. van den Bogaart, J.V. Guzmán, J.T. Mika, B. Poolman, On the mechanism of pore formation by melittin, J. Biol. Chem. 283 (2008) 33854–33857, https://doi.org/10.1074/jbc.M805171200.
[44] B. Bechinger, Structure and functions of channel-forming peptides: magainins, cecropins, melittin and alamethicin, J. Membr. Biol. 156 (1997) 197–211.
[45] H. Raghuraman, A. Chattopadhyay, Melittin: a membrane-active peptide with diverse functions, Biosci. Rep. 27 (2007) 189–223, https://doi.org/10.1007/s10540-006-9030-z.
[46] S. Macchi, G. Signore, C. Boccardi, C.D. Rienzo, F. Beltram, F. Cardarelli, Spontaneous membrane-translocating peptides: influence of peptide self-aggregation and cargo polarity, Sci. Rep. 5 (2015) 16914, , https://doi.org/10.1038/srep16914.
[47] R. Voltan, E. Rimondi, E. Melloni, G.M. Rigolin, F. Casciano, M.V. Arcidiacono, C. Celeghini, A. Cuneo, G. Zauli, P. Secchiero, Ibrutinib synergizes with MDM-2 inhibitors in promoting cytotoxicity in B chronic lymphocytic leukemia, Oncotarget 7 (2016) 70623.
[48] S. Ran, A. Downes, P.E. Thorpe, Increased Exposure of Anionic Phospholipids on the Surface of Tumor Blood Vessels, (2002), p. 10.
[49] M.-L. Jobin, P. Bonnafous, H. Temsamani, F. Dole, A. Grélard, E.J. Dufourc, I.D. Alves, The enhanced membrane interaction and perturbation of a cell penetrating peptide in the presence of anionic lipids: toward an understanding of its selectivity for cancer cells, Biochim. Biophys. Acta BBA Biomembr. 1828 (2013) 1457–1470, https://doi.org/10.1016/j.bbamem.2013.02.008.